Chemistry Africa (2019) 2:277–289
https://doi.org/10.1007/s42250-018-00035-w

ORIGINAL ARTICLE

# Inhibition of Carbon Steel Corrosion in 1 M $H_2SO_4$ Using Soy Polymer and Polyvinylpyrrolidone

S. C. Nwanonenyi[1,2] · H. C. Obasi[1] · I. C. Chukwujike[3] · M. A. Chidiebere[2] · E. E. Oguzie[2]

Received: 20 September 2018 / Accepted: 6 December 2018 / Published online: 17 December 2018


**Abstract**
The inhibition of carbon steel corrosion induced in 1 M $H_2SO_4$ by soy polymer (SP) from an extract of Glycine Mac-L and polyvinylpyrrolidone (PVP) respectively was investigated at 30–60 °C using hydrogen gas evolution, potentiodynamic polarization and quantum chemical computation technique respectively. Results obtained from hydrogen gas evolution technique revealed that SP and PVP respectively acted as an inhibitor for corrosion of carbon steel in 1 M $H_2SO_4$ solution. The increase in inhibition efficiency (IE%) of SP and PVP reached a maximum at 89.5% and 84.36% respectively, and the increment was found to be dependent on inhibitor concentration. The combination of mixture of SP and PVP as single inhibitor showed better inhibition improvement compared to individual inhibitor. Temperature study reveals that inhibition efficiency decreased with a rise in temperature suggesting physical adsorption. The computed parameters for the activation energies and heat of adsorption of the corrosion process supported the physical adsorption mechanism proposed. Regression analysis (adsorption isotherm model) was used to approximate the adsorption characteristics of the SP and PVP. Polarization data revealed that SP and PVP respectively adsorption acted as a mixed type inhibitor and also affected the anodic and cathodic partial reactions process. Quantum chemical computations were performed using the density functional theory to establish a clear link existing between the effectiveness of the inhibitor and its electronic properties.

**Keywords** Soy polymer · Polyvinylpyrrolidone · Carbon steel · Corrosion

## 1 Introduction

Carbon steel has wide application in the fabrication or designing of many engineering components in form of machine parts or tools, etc. [1] due to its inherent engineering properties. The integrity, safety and durability of some these components or machine tools are not guaranteed when exposed to unfavourable environment during service. For instance, the surface of either bare or coated carbon steel machine parts or tools, etc. becomes weak with time as a result of their limited corrosion resistance and continuous contact with aggressive solutions of mineral acids, especially when exposed to chemical treatment processes such as acid pickling, oil well acidizing, acid cleaning, textile dyeing, water treatment and industrial cleaning of metallic parts, tools, etc., [2]. In addition, the surface of the bare metal component parts tends to disintegrate, rust, corrode and crack resulting to wear and reverting to natural ore with time when exposed environment containing moisture; a technical process regarded as corrosion [3]. The process of metal corrosion is electrochemical in nature involving anodic and cathodic reaction respectively. Anodic reaction involves dissolution of metal whereas cathodic reaction involves hydrogen and oxygen reduction respectively. It is the combination of these reactions that constitute the destruction of metal and inherent properties associated with the metal. The consequences of metallic component failures in relation to corrosion are many and include the followings injuries, death, material loss, contamination and pollution, loss of time, mechanical and structural damage, etc. Hence, these negative effects can be regulated or controlled using various techniques to safeguard the metal from the aggressive

✉ S. C. Nwanonenyi
simeonnwanonenyi@gmail.com

[1] Department of Polymer and Textile Engineering, Federal University of Technology, Owerri, Nigeria

[2] Electrochemistry and Materials Science Research Laboratory, Department of Chemistry, Federal University of Technology, Owerri, Nigeria

[3] Department of Polymer and Textile Engineering, Nnamdi Azikiwe University, Awka, Nigeria

environments surrounding the surfaces. Among the various technical approaches that have been utilized in tackling the menace of metallic corrosion, the use of corrosion inhibitors is regarded as the most technical and effective means of regulating corrosion [3]. A corrosion inhibitor is regarded as a chemical substance which, when introduced or added in a little amount or quantity to a corrosive environment regulates the rate of metal dissolution. The corrosion inhibitors regulate dissolution of metal surfaces by being adsorbed on the surface of metals and forming a protective layer, which hinders access to corrosive species. This protective action of corrosion inhibitors is attributed to the presence of surface active functional groups and unique electron delocalization which facilitate the formation of rather stable metal-polymer complexes on the metal surfaces, which protect the metal surface from corrodent attack [4, 5]. Furthermore, a good corrosion inhibitor exhibits distinct characteristics such as hydrophobicity, safe in handling (non-toxic and biodegradable), renewable, low cost, stability, short and long-term durability in service, etc. [6, 7].

The search for corrosion inhibitor that exhibits the above stated properties emanates from organic or polymeric materials from the natural or synthetic background. Polymers are substances composed of macromolecules characterized by multiple repetitions of smaller molecules that are covalently bonded together to provide a set of properties. Some polymers either on their own or by the modification exhibit impermeability to different media, inherent stability, low cost, excellent chemical resistance, unusual deformation, short and long-term service durability, good metal corrosion resistance, etc. [8]. The use of green corrosion inhibitors derived from mainly natural polymers and organic substances has advocated considerable attention in the field of metal corrosion and protection due to growing global concerns on safeguarding the environment from toxic substances. It is interesting to know that a survey of the scientific literature reveals that many naturally occurring polymers (such as cellulose, tannic acid, lignin, chitosan, starch, gums etc.) as having been used effectively for different corrosion control applications [9]. This research area is of enormous importance and beneficial because of readily available of the soy polymers, their ability to degrade by biological means and pose no threat to the environment. In addition, it creates an avenue for diversification of the applications of the polymers. The molecular structure and the functionality of these polymers suggest their strong potential to become an effective corrosion inhibitor. Soy polymer is obtained from soybean which is a class of the beans family. It contains protein, carbohydrates, oil, vitamins and minerals, but protein forms the predominant part compared to other contents [10]. Protein has two functional groups (amino acid group, $NH_2$ and carboxyl acid group, COOH) in its molecular structure. Soy polymer from soybean forms a colloidal solution (sol) in water and consists of several aggregates of protein molecules which possess electric charges. Also, in water carboxylic group of protein molecules, forms of carboxylate ion (negative) whereas amino acid group forms to ammonium ion (positive) [11]. The pH variation of a protein determines whether the ammonium ion or carboxylate ion will predominate. The wide applications of soy polymer are seen in different industries such as cosmetics, papermaking, textile, food, pharmaceutical, etc. Applications of polyvinylpyrrolidone are widely seen in medicine, pharmacy, cosmetics and industrial products. It is used as an additive in coating, food additives and in personal care products, such as shampoos and toothpaste, in paints, adhesives, etc.

In considering the adsorption capability of corrosion inhibitors, some factors are considered which include: the type and charge on the metal surface, species (corrosive agents) present in the electrolyte and also, the molecular or electronic structure of the compound used as an inhibitor. It is apparent that soy polymer from soybean and polyvinylpyrrolidone are useful in this regard. Soy polymer (SP) and polyvinylpyrrolidone (PVP) are safe in handling and soluble in water. According to the constituents of the molecular structure of SP and PVP, it is obvious that SP and PVP are good metal corrosion inhibitors, and the polymers have shown to be effective corrosion inhibitors [10, 12]. However, further studies are required to investigate the carbon steel corrosion inhibition mechanism of SP and PVP respectively in the sulphuric acid environment.

It is, therefore, the objective of this study to investigate the behaviour of carbon steel in 1 M $H_2SO_4$ solution, advance the use safe polymeric inhibitors to regulate the corrosion of carbon steel, and report the inhibiting strength of SP, PVP and their mixtures on the corrosion of carbon steel in 1 M $H_2SO_4$ solution; to explain the ability the molecular inhibitive species of SP and PVP molecule has to act as corrosion inhibitor using density functional theory (DFT). The inhibiting effect of the polymers was determined using hydrogen evolution techniques and potentiodynamic polarization measurement.

## 2 Materials and Methods

### 2.1 Material Preparation

Materials used in this work include: soybean seeds and carbon steel sheet (obtained from local market in Nigeria), analytical grades of chemicals and reagents (polyvinylpyrrolidone, sulphuric acid, distilled water, ethanol and acetone), fine grade of abrasive paper.

Soybean seeds used were sorted to remove irrelevant materials, weighed, washed thoroughly with distilled water

and boiled for 30 min with distilled water. At the end of the stipulated time, the boiled water was removed and seeds were dehulled and dried at 60 °C in an oven. The dried seeds were toasted for 20 min at a temperature range of 70–100 °C, grounded using dry milling technique and sieved to a particle size of 20 µm to obtain a very fine powder of soy polymer.

Carbon steel sheet consisting of the following weight percent (0.101% C, 0.302% S, 0.171% Mn, 0.020% P, and 0.0020% S and Fe 99.5%) was mechanically press cut to coupon specifications of 3 × 3 × 0.2 cm dimension. The coupons were polished with a fine grade of abrasive paper, rinsed in acetone, degreased with ethanol, washed with distilled water, dried in hot air and kept in a desiccator.

Stock solutions of blank 1 M $H_2SO_4$ acid were prepared with distilled water using serial dilution principle. The inhibited solutions were prepared by dissolving 1.0–5.0 g of SP and PVP respectively with vigorous shaking in 1 L of 1 M $H_2SO_4$ solution.

### 2.2 Experimental Method

#### 2.2.1 Hydrogen Gas (Gasometric) Technique

This experimental method was used based on its relative rapidity in monitoring changes in metal corrosion and inhibition process caused by inhibitor with respect to evolution of gas in metal and corrodent systems within a short period. The gasometric evolution technique was used for the investigation of corrosion rates and inhibition of carbon steel in 1 M $H_2SO_4$ solution respectively using polymeric inhibitors. The prepared test solution was introduced into the conical flask fitted graded side-arm burette filled with paraffin oil as reported elsewhere [12] and placed in a thermostatically controlled water-bath at the stipulated temperature. When the test solution attained the desired temperature, prepared carbon steel coupon was immersed using plastic thread in the test solution. The course of corrosion reaction was carefully followed and monitored by recording the volume of hydrogen gas evolved as a function time. All the experiments were performed using different concentrations of test solutions at various temperatures (30–60 °C) and the results presented are the averages of three experimental runs.

### 2.3 Electrochemical Technique

Potentiodynamic polarization studies were conducted using a computer controlled electrochemical workstation (PARC-2273 Advanced Electrochemical Instrument). It has a conventional glass cell assembly that consists of a platinum plate (counter electrode), a saturated calomel electrode (reference electrode), and the carbon steel (working electrode). The carbon steel coupon was embedded in epoxy resin leaving a surface area of 1 $cm^2$ uncovered, immersed in the test solution using a coated copper wire for electrical contact. After establishing a steady state open circuit potential (OCP) at a stabilization period of 30 min, the potentiodynamic polarization measurements were conducted in the potential range of − 250 to + 250 mV relative to the corrosion potential of 0.333 mV/s scan rate. Each experiment was performed in triplicate and the average values of corrosion parameters obtained were presented.

### 2.4 Quantum Chemical Computation

The theoretical calculation was done based on the fact that the structure or geometry of molecules that determine the properties of the molecule [13–15]. Molecular modelling was performed to calculate the different molecular electronic parameters of the inhibitor in order to understand the behaviour of adsorption of molecular inhibitive species of the inhibitor on the carbon steel surface. DFT electronic program Dmol3 was used to calculate the following parameters; the energy of the lowest unoccupied molecular orbital $E_{(LUMO)}$, the energy of the highest occupied molecular orbital $E_{(HOMO)}$ and energy gap $\Delta E$ ($E_{HOMO} - E_{LUMO}$). The electronic parameters for the modelling include Mulliken population analysis, unrestricted spin polarization-DND basis set and the Perdew–Wang (PW) local correlation density functional.

### 2.5 Regression Analysis (Adsorption Isotherms)

The adsorption isotherms (regression models) were used to study the inhibition adsorption process, that is, to determine the mode of inhibition adsorption for the corrosion reaction process. Also, it was done to present the importance of using regression models and its methodology in interpreting corrosion inhibition results [16–19]. Regression isotherm models used in the research include; Temkin, Freundlich and Langmuir adsorption isotherm.

## 3 Results and Discussion

### 3.1 Hydrogen Gas Evolution and Corrosion Rate

Hydrogen gas evolution measurement was used to study the corrosion of carbon steel coupons in 1 M $H_2SO_4$ in the absence and presence of SP and PVP as inhibitors respectively. The effectiveness and suitability of the hydrogen evolution technique in monitoring the progress of corrosion inhibition reaction with respect to the evolution of gas in metal and corrodent systems have been established elsewhere [21–23]. It was observed that the corrosion reaction process was characterized by the rapid bubbles from the hydrogen gas released and material loss due to corrosion

rates. The plots of hydrogen gas evolution against time for carbon steel corrosion in 1 M $H_2SO_4$ in the absence and presence of SP and PVP as inhibitors, respectively at 30–60 °C are shown in Fig. 1a–d respectively. The volume of hydrogen gas released at higher temperature was much compared to those released at lower temperatures as seen from the plots. Also, the report from the plots confirmed that there is no incubation period (time interval required for the corrodent to break down the oxide film on the carbon steel surface) observed during the reaction process. That is, the release of hydrogen gas commenced immediately the metal came in contact with corrodent, though the volume of hydrogen gas released varies with the reaction time in a linear manner. The hydrogen bubbles observed were released from the cathodic area or surface of the metal whereas metal dissolution occurred at the anodic area. Furthermore, the plots

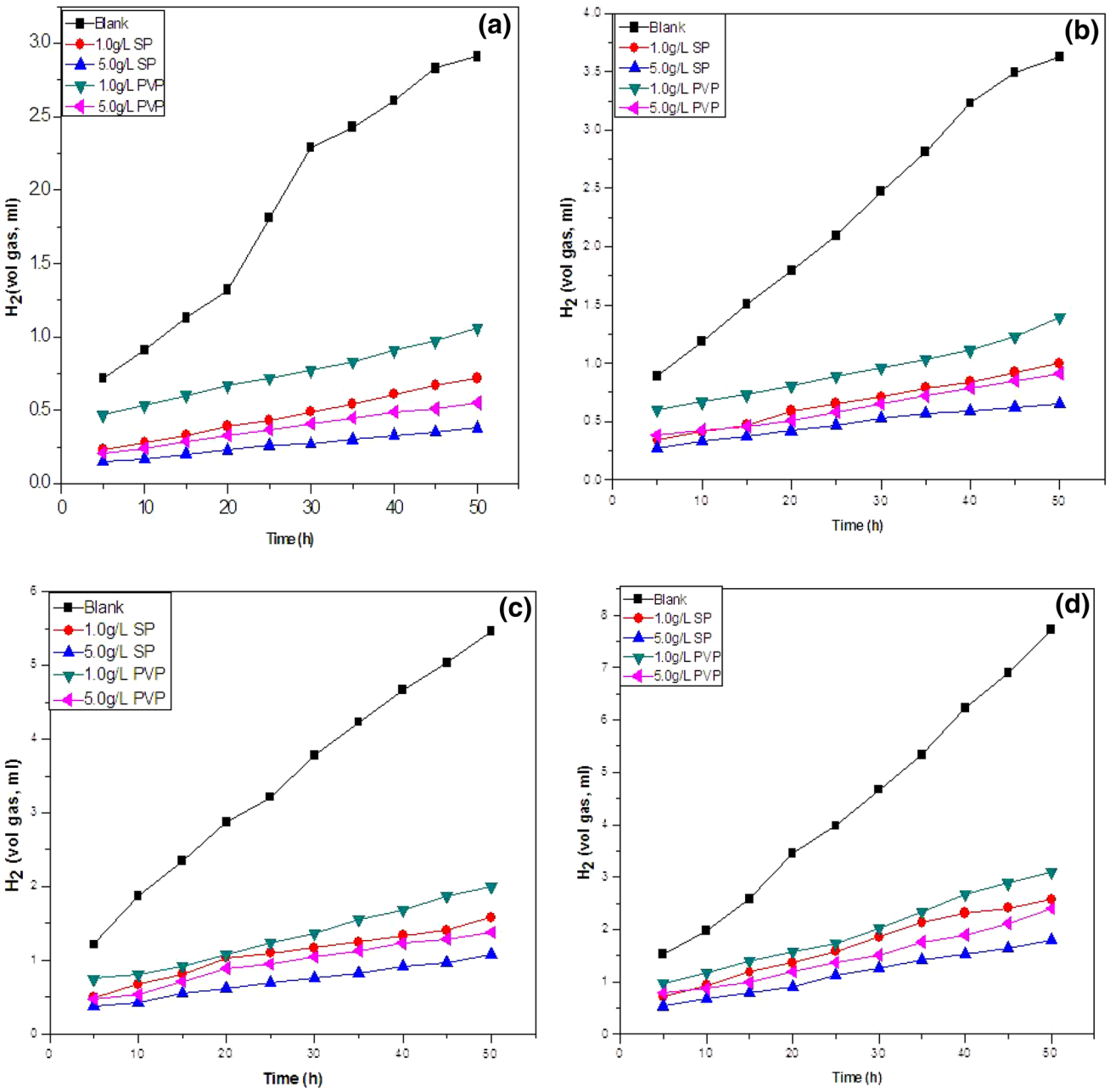


**Fig. 1** **a** Hydrogen gas evolution during carbon steel corrosion in 1 M $H_2SO_4$ at 30 °C in absence and presence of SP and PVP. **b** Hydrogen gas evolution during carbon steel corrosion in 1 M $H_2SO_4$ at 40 °C in absence and presence of SP and PVP. **c** Hydrogen gas evolution during carbon steel corrosion in 1 M $H_2SO_4$ at 50 °C in absence and presence of SP and PVP. **d** Hydrogen gas evolution during carbon steel corrosion in 1 M $H_2SO_4$ at 60 °C in the absence and presence of SP and PVP

illustrate that on the introduction of the inhibitors into the corrodent the volume of hydrogen gas released decreased, indicating that the inhibitors actually offer inhibition to corrosion of carbon steel in 1 M $H_2SO_4$ environment.

It is evident from the plots that SP exhibited better inhibitive performance compare to PVP for corrosion of carbon steel in 1 M $H_2SO_4$ in both low and high inhibitor concentration. This could be attributed to the presence of better inhibitive species within the SP molecules which formed a protective complex layer on the metal surface during continual contact between metal/inhibitor-corrodent systems [24]. The volume of hydrogen gas released was observed to decrease with increasing concentrations of SP and PVP, suggesting that their inhibiting performance of the polymers also depends on the concentration.

The hydrogen gas evolution rate can be correlated to corrosion rate because the amount of hydrogen gas released depicts the extent of corrosion damage done on the metal surface [14]. Based on that, the corrosion rate ($CR_H$) is obtained from the relation between the hydrogen gas evolved and the time interval of evolution according to the expression [24] stated below:

$$CR_H = \frac{V_t - V_i}{t_t - t_i} \quad (1)$$

where $V_t$ and $V_i$ represent the volumes of hydrogen evolved at time $t_t$ and $t_i$ respectively.

The values of the corrosion rate ($CR_H$) were computed according to Eq. (1) and presented in Table 1. The results illustrate that corrosion rates increased with the rise in temperature and reduced in the presence of SP and PVP respectively compared to the blank solution. Further inspection of the table reveals that carbon steel is observed to exhibit a higher corrosion rate in the presence of PVP compared to SP. At the end of 50 h exposure of carbon steel coupon in the sulphuric solution, corroded product on the surface of coupon exposed in the blank solution was large compared to those on inhibited solution. Also, the corroded product was dark brown in colour.

## 3.2 Inhibition Efficiency

The efficacy of inhibitor in safeguarding or protecting metal surfaces during acid induced corrosion is dependent on the ability of the molecular inhibitive species of the inhibitor to be adsorbed on the metal surface and the ability of the resulting adsorbed film to disengage the metal surface from the corrodent medium [17]. If it is believed that in inhibited solution corrosion occurs on the remaining free surfaces after some sites have been barricaded effectively by the adsorbed inhibitor film such that the covered surfaces have negligible rates of corrosion, the degree of surface coverage (θ) and inhibition efficiency (%I) can be computed according to the following Eqs. (2 and 3) stated below [25]:

$$\theta = \frac{CR_{H2} - CR_{H1}}{CR_{H2}} \quad (2)$$

$$\%I = \left[\frac{CR_{H2} - CR_{H1}}{CR_{H2}}\right] \times 100 \quad (3)$$

where $CR_{H2}$ and $CR_{H1}$ represent the corrosion rates in the absence and presence of inhibitor (SP and PVP) respectively as determined from rates of hydrogen gas evolved. The calculated values of inhibition efficiency (%I) and degree of surface coverage (θ) are illustrated in Table 1. The results indicate that both SP and PVP exhibited good inhibition efficiency during the corrosion of carbon steel in 1 M $H_2SO_4$. It is assumed that the inhibitive performance of the inhibitors is due to adsorption of SP and PVP respectively on the carbon steel surface which reduced the surface area available

**Table 1** Calculated values of corrosion rates, inhibition efficiency, and degree of surface coverage for carbon steel in 1 M $H_2SO_4$ at 30–60 °C from hydrogen gas evolution measurement in the absence and presence of SP and PVP

| System (g/L) | Corrosion rate ($CR_H$) ($H_2$ gas vol mL/h) × $10^{-2}$ | | | | Inhibition efficiency (%I) | | | | Degree of surface coverage (θ) | | | |
|---|---|---|---|---|---|---|---|---|---|---|---|---|
| | 30 °C | 40 °C | 50 °C | 60 °C | 30 °C | 40 °C | 50 °C | 60 °C | 30 °C | 40 °C | 50 °C | 60 °C |
| Blank | 4.86 | 6.09 | 9.14 | 13.75 | – | – | – | – | – | – | – | – |
| 1.0SP | 1.09 | 1.47 | 2.43 | 4.11 | 77.57 | 75.86 | 73.41 | 70.11 | 0.78 | 0.76 | 0.73 | 0.70 |
| 2.0SP | 0.94 | 1.36 | 2.26 | 3.85 | 80.66 | 77.67 | 75.27 | 72.00 | 0.81 | 0.78 | 0.75 | 0.72 |
| 3.0SP | 0.80 | 1.17 | 2.07 | 3.57 | 83.54 | 80.79 | 77.38 | 74.04 | 0.84 | 0.81 | 0.77 | 0.74 |
| 4.0SP | 0.69 | 1.02 | 1.81 | 3.23 | 85.80 | 83.25 | 80.20 | 76.51 | 0.86 | 0.83 | 0.80 | 0.77 |
| 5.0SP | 0.51 | 0.85 | 1.53 | 2.79 | 89.51 | 86.04 | 83.26 | 79.71 | 0.90 | 0.86 | 0.83 | 0.80 |
| 1.0 PVP | 1.31 | 1.75 | 2.79 | 4.71 | 73.05 | 71.26 | 69.47 | 65.75 | 0.73 | 0.71 | 0.69 | 0.66 |
| 2.0 PVP | 1.17 | 1.63 | 2.63 | 4.45 | 75.93 | 73.23 | 71.23 | 67.64 | 0.76 | 0.73 | 0.71 | 0.68 |
| 3.0 PVP | 1.03 | 1.51 | 2.45 | 4.15 | 78.40 | 75.40 | 73.19 | 69.82 | 0.78 | 0.75 | 0.73 | 0.70 |
| 4.0 PVP | 0.93 | 1.39 | 2.27 | 3.91 | 80.86 | 77.18 | 75.16 | 71.56 | 0.81 | 0.77 | 0.75 | 0.72 |
| 5.0 PVP | 0.76 | 1.19 | 2.03 | 3.57 | 84.36 | 80.46 | 77.79 | 74.04 | 0.84 | 0.80 | 0.78 | 0.74 |

for corrosion. Also, the level of protection increases with an increase in inhibitor concentration due to the higher degree of surface coverage emanating from enhanced inhibitor adsorption but decreases with a rise in temperature. Hence, the decrease in inhibition efficiency with the rise in temperature is suggestive of physical adsorption mechanism [24].

## 4 Regression Analysis (Adsorption Isotherms)

The protective film on the metal surface resulting from the adsorption of the inhibitor on the surface during acid induced corrosion regulates the corrosive effect on the metal surface by either homogenous or heterogenous layer adsorption [12]. The adsorption isotherm model (regression model) based on the degree of surface coverage data provides the information about the interactions between the inhibitor molecules themselves as well as their interactions with the metal surface [25]. The values of the degree of surface coverage (θ) evaluated from hydrogen gas evolution measurement using Eq. (2) were fitted into different adsorption isotherms and the correlation coefficient ($R^2$) obtained establish best results. The adsorption isotherms model used are expressed according to Eqs. (4), (5) and (6) respectively stated below [26]:

$$\frac{C}{\theta} = \frac{1}{K_{ads}} + C \quad \text{(Langmuir)} \tag{4}$$

$$In\theta = InK_{ads} + nInC \quad \text{(Freundlich)} \tag{5}$$

$$\exp(-2n\theta) = K_{ads}C \quad \text{(Temkin)} \tag{6}$$

where, C = concentration of inhibitor, $K_{ads}$ = adsorption equilibrium constant, θ = degree of surface coverage, n = molecular interaction parameter, (0 < n < 1).

The plots of the Langmuir (C/θ against C), Freundlich (In θ against InC) and Temkin (θ against InC) adsorption isotherms respectively were performed and Fig. 2 presents the plot of Langmuir isotherm adsorption. Linearity was obtained in all the Langmuir plots of Fig. 2 with good correlation coefficient, thus suggesting proper adsorption of SP and PVP respectively on carbon steel surface. Also, the adsorption parameters obtained were presented in Table 2. In addition, the results of Table 2 reveal that the adsorption of molecules of SP and PVP respectively on the surface of carbon steel followed Langmuir adsorption isotherm. This is because the correlation coefficient ($R^2$) of Langmuir adsorption isotherm obtained is closer to unity compared to other adsorption isotherms. From the table, it is seen clearly that values of $K_{ads}$ obtained for both SP and PVP are positive, and SP has higher values than those of PVP at 30–60 °C, thus suggesting that SP showed better inhibition than PVP [26].

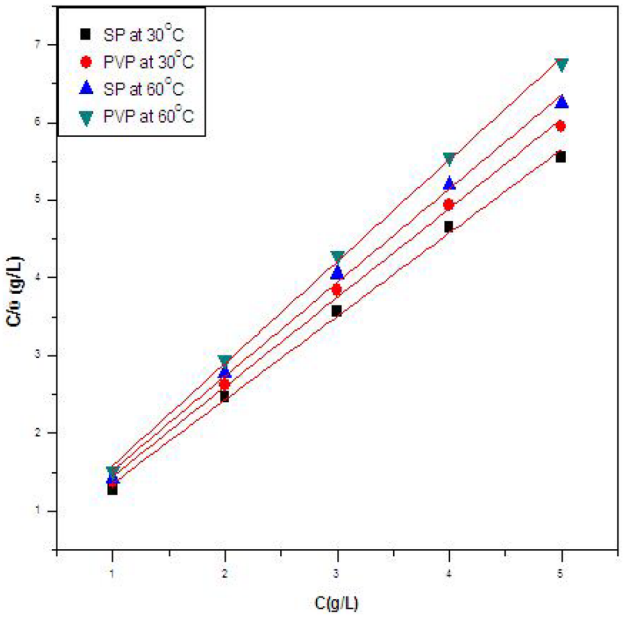


**Fig. 2** Langmuir Adsorption isotherm for corrosion inhibition of SP and PVP on carbon steel in 1 M $H_2SO_4$ at 30 °C and 60 °C

The adsorption equilibrium constant, $K_{ads}$ computed from the intercepts of the plots is related to Gibb's free energy of adsorption, $\Delta G_{ads}$ according to Eq. (7) stated below:

$$K_{ads} = \frac{1}{55.5}\exp\left[\frac{-\Delta G_{ads}}{RT}\right] \tag{7}$$

The calculated values of $\Delta G_{ads}$ were found to be −13.26 kJ/mol and −14.25 kJ/mol at 30 and 60 °C respectively for SP. $\Delta G_{ads}$ values of −13.10 kJ/mol and −14.18 kJ/mol were obtained for PVP at 30 °C and 60 °C respectively. These $\Delta G_{ads}$ values obtained to support the physical adsorption of SP and PVP respectively on the carbon steel surface [27] and also the negative values of $\Delta G_{ads}$ obtained are evidence of spontaneous and strong adsorption of the SP and PVP respectively on the carbon steel surface [28–31].

## 5 Effect of SP and PVP Mixture as Corrosion Inhibitor

The improvement in the effectiveness of the inhibitor by combining two or more materials as a single corrosion inhibitor has been made available in the scientific literature by many researchers [12, 20, 25, 32, 33]. This enhancement in inhibitor effectiveness is attributed to synergistic effect due to the availability of more adsorption centres within the inhibitor. The adsorption centres (functional groups) of the inhibiting molecule form complex ions

**Table 2** Calculated adsorption parameters for corrosion inhibition of SP and PVP on carbon steel in 1 M $H_2SO_4$ at 30 °C and 60 °C

| System | Temp (°C) | Slope | Intercept | $K_{ads}$ | $R^2$ | Isotherm |
|---|---|---|---|---|---|---|
| SP | 30 | 1.0729 | 0.2872 | 3.4819 | 0.9970 | Langmuir |
| | 60 | 1.2060 | 0.3231 | 3.0950 | 0.9967 | |
| PVP | 30 | 1.1471 | 0.3062 | 3.2658 | 0.9972 | |
| | 60 | 1.3098 | 0.3316 | 3.0157 | 0.9984 | |
| SP | 30 | 0.0840 | − 0.2584 | 0.7723 | 0.9256 | Freundlich |
| | 60 | 0.0795 | − 0.3762 | 0.6865 | 0.8741 | |
| PVP | 30 | 0.0834 | − 0.3241 | 0.7232 | 0.9266 | |
| | 60 | 0.0695 | − 0.4241 | 0.6544 | 0.9390 | |
| SP | 30 | 0.0700 | 0.7710 | 0.9475 | 0.9111 | Temkin |
| | 60 | 0.0651 | 0.7217 | 0.9541 | 0.9131 | |
| PVP | 30 | 0.0592 | 0.6894 | 0.9600 | 0.8594 | |
| | 60 | 0.0484 | 0.6536 | 0.9689 | 0.9298 | |

with a metal surface which provides blanketing or protective film effect that safeguards the metal surface within the corrodent system. In this research SP and PVP were combined in different proportions as corrosion inhibitor and the effect was tested on the corrosion inhibition of carbon steel in 1 M $H_2SO_4$ at different temperatures. The results obtained as shown in Table 3 evidence that mixture of SP and PVP at different proportions enhanced the inhibiting characteristics of the combined inhibitor (SP and PVP) compared to individual polymeric inhibitors. This improvement suggests a possible role played by the availability of more inhibiting species existing within the combined inhibitor structure. Hence, it is an indication that the degree of surface coverage exhibited by the combination of SP and PVP as a corrosion inhibitor increased. Furthermore, it is observed that the corrosion rate of carbon steel in 1 M $H_2SO_4$ appears higher in individual inhibitors compared to the inhibitive effectiveness of the inhibitor produced by combining SP and PVP. Thus, suggesting that synergistic interactions obtained from the combined inhibitor enhanced the stability of the insoluble adsorbed protective film formed between the inhibitor and corrosion product at a lower temperature. However, at a higher temperature, the adsorbed protective film begins to dissolve with a resultant reduction in the effectiveness of combined action of SP and PVP, and more increment in the metal destruction.

## 6 Temperature Effect

The effect of temperature on the corrosion inhibition of SP and PVP respectively on carbon steel in 1 M $H_2SO_4$ was studied at 30–60 °C to determine the dependence of inhibitor's efficiency on temperature and corrosion behaviour of carbon steel in 1 M $H_2SO_4$ in the presence of SP and PVP respectively. The results obtained as shown in Table 1 reveal that the rates of carbon steel corrosion in 1 M $H_2SO_4$ in the absence and presence of SP and PVP respectively increased with the rise in temperature but the inhibition efficiency decreased. The high rate of dissolution of carbon steel in 1 M $H_2SO_4$ solution observed at elevated temperature could be attributed to more dissolution energy effect acquired by the corrosive agent within the aggressive medium. Also, the desorption of adsorbed inhibitor due to enhanced solution agitation by higher rates of hydrogen gas evolution at elevated temperature is possible and may cause the ability of the inhibitor to be adsorbed on the carbon steel surface to

**Table 3** Effect of SP and PVP mixture as inhibitor on corrosion of carbon steel corrosion in 1 M $H_2SO_4$ at 30–60 °C

| System (g/L) | Corrosion rate ($CR_H$) ($H_2$ gas vol mL/h) × $10^{-2}$ | | | | Inhibition efficiency (%I) | | | | Degree of surface coverage (θ) | | | |
|---|---|---|---|---|---|---|---|---|---|---|---|---|
| | 30 °C | 40 °C | 50 °C | 60 °C | 30 °C | 40 °C | 50 °C | 60 °C | 30 °C | 40 °C | 50 °C | 60 °C |
| Blank | 4.86 | 6.09 | 9.14 | 13.75 | – | – | – | – | – | – | – | – |
| 3.0 SP | 0.80 | 1.17 | 2.07 | 3.57 | 83.54 | 80.79 | 77.38 | 74.04 | 0.84 | 0.81 | 0.77 | 0.74 |
| 3.0SP + 0.5PVP | 0.67 | 1.09 | 1.88 | 3.41 | 86.21 | 82.10 | 79.43 | 75.20 | 0.86 | 0.82 | 0.79 | 0.75 |
| 3.0SP + 1.0PVP | 0.52 | 1.01 | 1.79 | 3.29 | 89.09 | 83.42 | 80.42 | 76.07 | 0.89 | 0.83 | 0.80 | 0.76 |
| 3.0SP + 1.5PVP | 0.32 | 0.94 | 1.72 | 3.15 | 93.42 | 84.56 | 81.18 | 77.09 | 0.93 | 0.86 | 0.81 | 0.77 |
| 3.0SP + 2.0PVP | 0.19 | 0.83 | 1.60 | 2.99 | 96.09 | 86.37 | 82.49 | 78.25 | 0.96 | 0.86 | 0.82 | 0.78 |

reduce [17]. In addition, this corrosion behaviour of carbon steel observed in 1 M $H_2SO_4$ in the presence of SP and PVP respectively suggests physical adsorption of the SP and PVP on the corroding carbon steel surface [24].

To evaluate the dependence of corrosion rate and inhibition efficiency on temperature two kinetic parameters (activation energies, $E_a$ and heat of adsorption, $Q_{ads}$) was employed. Arrhenius equation was used to compute the activation energies for the corrosion process in the absence and presence of the inhibitor according to Eq. (8) stated below:

$$\mathrm{Log}\frac{CR_2}{CR_1} = \frac{E_a}{2.303R}\left(\frac{1}{T_1} - \frac{1}{T_2}\right) \tag{8}$$

where $CR_1$ and $CR_2$ are the corrosion rates at temperatures $T_1$ and $T_2$ respectively. The calculated values of activation energies, $E_a$ were presented in Table 4. The results of the table reveal that in the presence of both SP and PVP in 1 M $H_2SO_4$ activation energy increased, thus leading to a reduction in the rates of corrosion of carbon steel. It has been reported that adsorption of the inhibitor on the metal surface can regulate the rate of dissolution by either reducing the available dissolution area (geometric blocking effect) or by modifying the electrochemical reactions occurring at the metal surface/inhibited solution interface during the inhibition corrosion process [34]. The experimental observations suggest that regulation of carbon steel dissolution in 1 M $H_2SO_4$ by SP and PVP respectively occurred mainly through physical adsorption of the inhibitors on the metal surface. Also, it suggests that the inhibitors did not modify the rate determining hydrogen adsorption steps of the dissolution process, but deactivated the recombination of a hydrogen atom on the carbon steel surface [21, 35].

**Table 4** Calculated values of activation energy (Ea) and heat of adsorption (Qads) for carbon steel corrosion in 1 M $H_2SO_4$ in the presence of SP and PVP as inhibitor at 30–60 °C

| System | Activation energy (KJ/mol) | Heat of adsorption (KJ/mol) |
|---|---|---|
| | 30–60 °C | 30–60 °C |
| Blank (1 M $H_2SO_4$) | 29.09 | – |
| 1.0 g/L SP | 37.12 | 11.70 |
| 2.0 g/L SP | 39.44 | 14.14 |
| 3.0 g/L SP | 41.84 | 17.12 |
| 4.0 g/L SP | 43.17 | 19.98 |
| 5.0 g/L SP | 47.53 | 22.67 |
| 1.0 g/L PVP | 35.79 | 9.27 |
| 2.0 g/L PVP | 37.36 | 11.15 |
| 3.0 g/L PVP | 38.98 | 11.70 |
| 4.0 g/L PVP | 40.17 | 14.14 |
| 5.0 g/L PVP | 43.27 | 17.12 |

The heat of adsorption ($Q_{ads}$) for the corrosion process was obtained from the trend of the degree of surface the coverage with temperature according to Eq. (9) stated below:

$$Q_{ads} = 2.303R\left[\log\left(\frac{\theta_2}{1-\theta_2}\right) - \log\left(\frac{\theta_1}{1-\theta_1}\right)\right] \times \frac{T_1T_2}{T_2 - T_1} \tag{9}$$

where $\theta_1$ and $\theta_2$ represent the degrees of surface coverage at temperature $T_1$ and $T_2$. The calculated values of heat of adsorption parameters are given in Table 3. The values of $Q_{ads}$ obtained bear negative signs, thus indicating that degree of surface coverage decreased with increase in temperature and this behaviour evidently supported the physical mechanism of adsorption earlier proposed [36].

## 7 Potentiodynamic Polarization Measurements

Polarization measurement was conducted to establish the effectiveness of SP and PVP respectively in altering the corrosion reaction of carbon steel induced in 1 M $H_2SO_4$. In addition, to evaluate the specific role played by SP and PVP respectively either as anodic, cathodic or mixed inhibitor during the corrosion inhibition of carbon steel in 1 M $H_2SO_4$. The changes observed in the anodic and cathodic polarization curves of carbon steel induced in 1 M $H_2SO_4$ in the absence and presence of a low and high concentration of SP and PVP were illustrated in Fig. 3a, b respectively. Also, the polarization parameters, corrosion potential ($E_{corr}$), corrosion current densities ($i_{corr}$), cathodic Tafel slope ($b_c$) and anodic Tafel slope ($b_a$) obtained from the polarization curves are presented in Table 5. Evidently, it is seen from the figures that the corrosion potential ($E_{corr}$) show more pronounced displacement towards a positive direction with a significant decrease in the current densities upon addition of SP whereas the addition of PVP pushed corrosion potential ($E_{corr}$) towards the negative direction with a resultant decrease in the current densities ($i_{corr}$). This behaviour suggests that the SP exhibited a more retarding effect on the anodic dissolution reaction compared to cathodic hydrogen gas evolution reaction while PVP retarded cathodic reaction more compared to the anodic reaction. The variations observed in the displacement of the corrosion potential ($E_{corr}$) by SP and PVP could be attributed to their different inhibitory species present in the molecular structure. In addition, it is suggested that both SP and PVP acted as mixed inhibitors based on the fact the displacement in corrosion potential caused by the addition of SP and PVP respectively does not exceed 85 mV [37]. The inhibition efficiency (IE%) was computed from the values of corrosion current density without ($i_{corr,\ bl}$) and with HPC ($i_{corr,\ inh}$) using the equation stated below as follows:

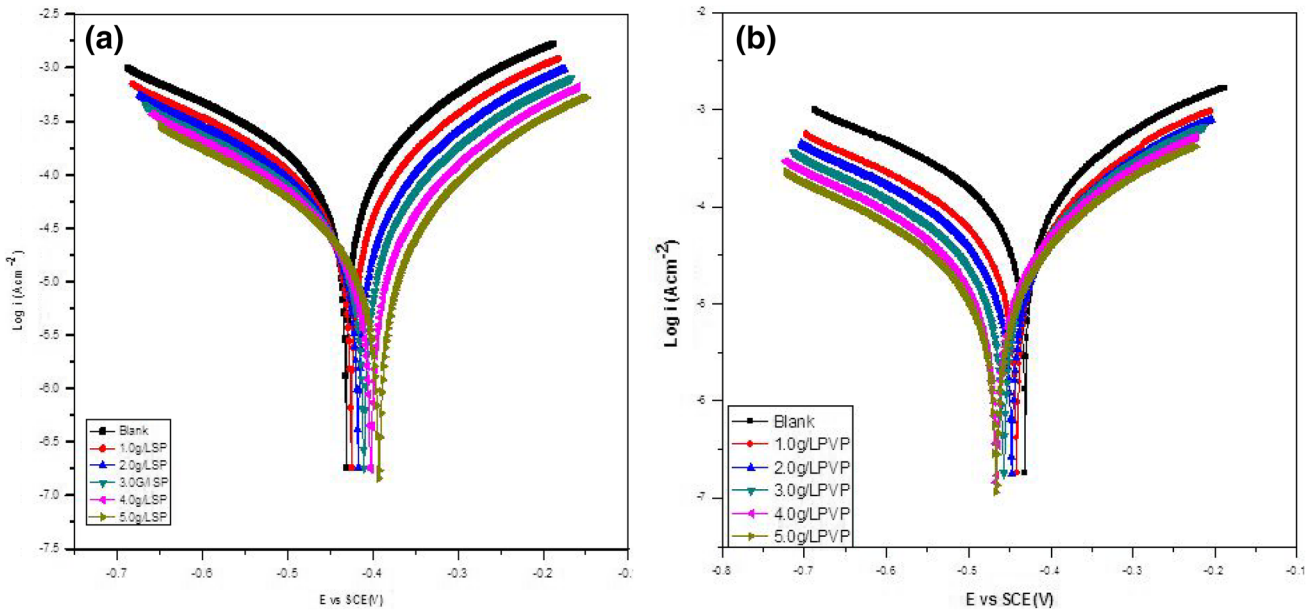


**Fig. 3** **a** Polarization curves of carbon steel corrosion in 1 M $H_2SO_4$ solution at 30 °C for different concentrations of SP. **b** Polarization curves of carbon steel corrosion in 1 M $H_2SO_4$ solution at 30 °C for different concentrations of PVP

**Table 5** Potentiodynamic polarization parameters for carbon steel corrosion in 1 M $H_2SO_4$ at different concentrations of SP and PVP at 30 °C

| System | $E_{corr}$ E [mV(SCE)] | $I_{corr}$ (μAcm$^{-2}$) | IE (%) | $B_c$ (mVdec$^{-1}$) | $B_a$ (mVdec$^{-1}$) |
|---|---|---|---|---|---|
| Blank | − 430.04 | 766.04 | – | 110.23 | 67.45 |
| 1.0 g/L SP | − 422.18 | 365.45 | 52.29 | 104.45 | 55.35 |
| 2.0 g/L SP | − 417.63 | 305.89 | 60.07 | 101.63 | 58.04 |
| 3.0 g/L SP | − 413.24 | 219.41 | 71.36 | 90.56 | 51.87 |
| 4.0 g/L SP | − 409.06 | 177.56 | 76.82 | 96.11 | 46.36 |
| 5.0 g/L SP | − 405.56 | 146.08 | 80.93 | 93.56 | 42.08 |
| 1.0 g/L PVP | − 435.56 | 727.78 | 36.46 | 123.67 | 93.11 |
| 2.0 g/L PVP | − 440.17 | 625.73 | 45.37 | 117.03 | 89.09 |
| 3.0 g/L PVP | − 452.26 | 516.18 | 54.94 | 109.12 | 90.89 |
| 4.0 g/L PVP | − 468.05 | 423.56 | 63.02 | 106.45 | 88.79 |
| 5.0 g/L PVP | − 479.38 | 313.89 | 72.60 | 101.78 | 85.06 |

$$IE\% = \left[\frac{i_{corr,\,bl} - i_{corr,\,inh}}{i_{corr,\,bl}}\right] \times 100 \quad (10)$$

## 8 Quantum Chemical Computation Result

The computed optimized electronic molecular structure of the inhibitors (protein and polyvinylpyrrolidone) including the HOMO orbital and LUMO orbital are illustrated in Figs. 4a–c and 5a–c respectively. Table 6 presents the calculated quantum chemical properties related to the electronic molecular structure of the most stable conformation of the protein and polyvinylpyrrolidone molecule respectively.

The interaction between the frontier orbital of the reactant molecules (as in the interaction metal and inhibitor in the presence of corrodent) necessitates the transition of electrons according to the Frontier Orbital Theory. $E_{HOMO}$ designates the potency of a molecule to donate electron(s) to an appropriate acceptor that possess low empty molecular orbital energy, whereas $E_{LUMO}$ indicates the ability of a molecule to accept electron(s). In addition, an increase in the $E_{HOMO}$ values is linked to improvement in the performance of molecular adsorption as well as the efficiency of the inhibition while low $E_{HOMO}$ values is a sign of the willingness of molecule to accept electron(s) with ease [38]. Hence, values of $E_{HOMO}$ obtained for protein

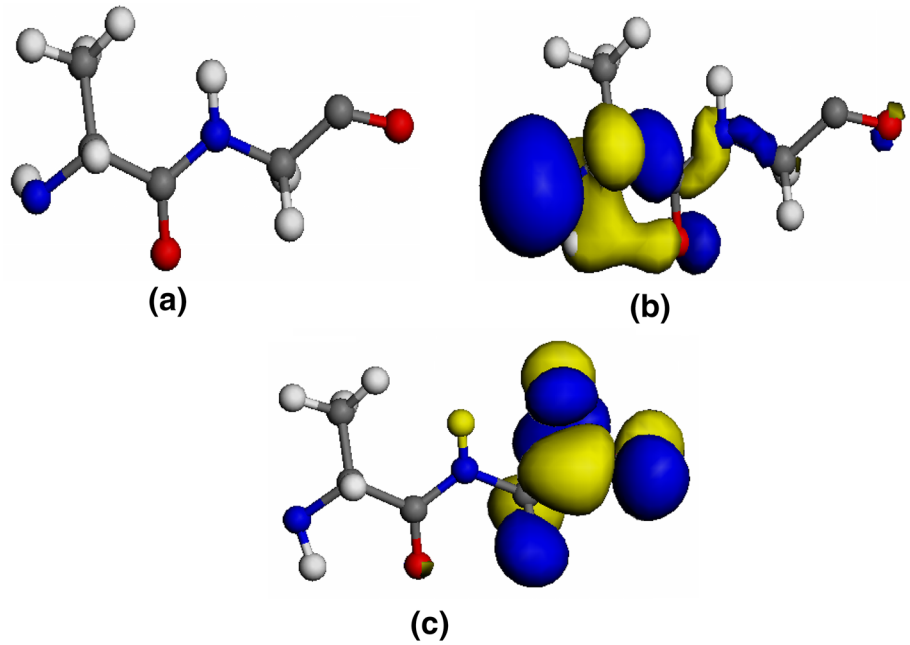


**Fig. 4** Molecular electronic structure of a protein unit: **a** optimized structure **b** HOMO orbital **c** LUMO orbital (atomic legend: gray = C; white = H; blue = N; red = O) (color figure online)

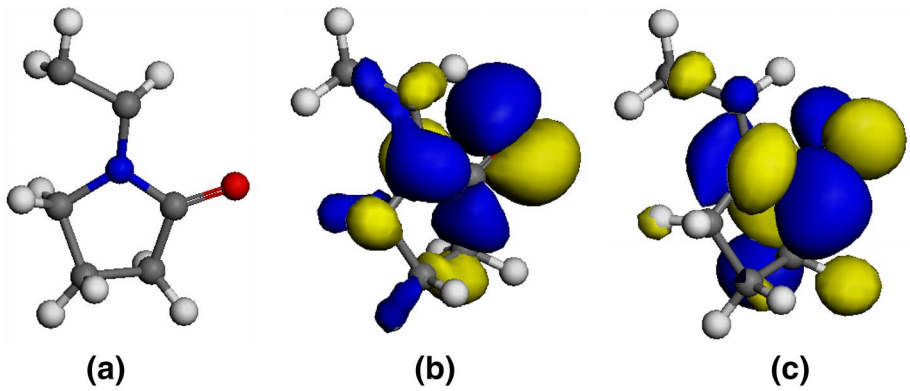


**Fig. 5** Molecular electronic structure of a polyvinylpyrrolidone unit: **a** optimized structure **b** HOMO orbital **c** LUMO orbital (atomic legend: gray = C; white = H; blue = N; red = O) (color figure online)

**Table 6** Calculated values of some quantum chemical parameters of protein and polyvinylpyrrolidone molecule

| Parameters | Protein values | Polyvinylpyrrolidone values |
|---|---|---|
| $E_{HOMO}$ (eV) | − 5.350 | − 5.441 |
| $E_{LUMO}$ (eV) | − 1.686 | − 0.193 |
| ΔE (eV) | − 3.664 | − 5.248 |
| I (eV) | 5.350 | 5.441 |
| A (eV) | 1.686 | 0.193 |
| χ (eV) | 3.518 | 2.817 |
| μ (eV) | − 3.518 | − 2.817 |
| η (eV) | 1.832 | 2.624 |
| ΔN (eV) | 0.950 | 0.797 |

and polyvinylpyrrolidone molecule are − 5.350 eV and − 5.441 eV respectively. This suggests a strong tendency towards the donation of electrons to the metal surface with the expectation of appreciable corrosion inhibition by the polymeric inhibitors. $E_{LUMO}$ values obtained for protein and polyvinylpyrrolidone molecule are − 1.686 eV and − 0.193 eV respectively, thus indicating the propensity of the inhibitor molecule to except electron(s) Also, low energy gap value (ΔE) affords good inhibition effectiveness because the energy of excitation needed to remove an electron from the last occupied orbital will be low [38]. The location of the HOMO orbital in a protein molecule is seen around the amino acid group and carboxyl acid group, suggesting the site preferred for the electrophilic attack through the molecule can interact with the metal surface. Probably, it is that of the molecule that has a high HOMO density which was oriented to the metal surface and adsorption of the molecule could be sharing of lone

pairs and the π-electrons of the carbonyl group. On the other hand, LUMO orbital domiciled around the carboxylic group and thus indicating the site for the nucleophilic attack which can accept an electron from the 3d-orbital of the iron atom to form feedback bond and strengthens the interaction between protein molecule and carbon steel surface.

In the case of polyvinylpyrrolidone molecule, the HOMO and LUMO orbitals are located around the vinyl and pyrrolidone group respectively. These are sites at which both the electrophilic and nucleophilic attacks can occur within the molecule. The relationship between the energies of HOMO and LUMO orbitals and ionization potential and electron affinity of the inhibitor molecule, respectively according to Koopman's theorem is established in the expressions stated below [39, 40]:

$$I = -E_{HOMO}. \tag{11}$$

$$A = -E_{LUMO}. \tag{12}$$

The absolute hardness (η) and electronegativity (χ) of the inhibitor molecule are calculated in terms of $E_{HOMO}$ and $E_{LUMO}$ according to Martinez and Stagljar [40]:

$$\eta = \frac{I - A}{2}. \tag{13}$$

$$\chi = \frac{I + A}{2}. \tag{14}$$

During the interaction between the metal surface and inhibitor, there is a transfer of electrons from the inhibitor to the d-orbital of the metal. The fraction of electrons transferred (ΔN) can be calculated using the expression stated below:

$$\Delta N = \frac{\chi_{Fe} - \chi_{inh}}{2(\eta_{Fe} - \eta_{inh})} \tag{15}$$

where $\chi_{Fe}$ (a theoretical electronegativity value of) = 7.0 eV for iron and $\eta_{Fe}$ (absolute hardness) = 0 is assumed, since I equals A for bulk metals [38]. Lukovits et al. [41] reported that if ΔN is less than 3.6, electron donating capability of the inhibitor will rise at the metal surface with the increase in the inhibition of efficiency. The values of ΔN obtained in this study for protein and polyvinylpyrrolidone molecules are 0.950 eV and 0.797 eV respectively, thus suggesting that protein and polyvinylpyrrolidone molecules respectively were a donor of electrons whereas carbon steel surface was the acceptor. In addition, the low value of dipole moment (μ) obtained for protein and polyvinylpyrrolidone molecule, respectively is an indication that molecules of the inhibitor exhibit hydrophobic character which favours the accumulation of the inhibitor molecules on the carbon steel surface [38].

## 9 Inhibition Mechanism

The rate at which metal corrodes and inhibited is dependent on the following factors nature of metal, corroding environment, inhibitor, corrodent, etc. [12]. During the corrosion process, it is believed that inhibitors regulate the dissolution of metal in the corrodent medium through adsorption at the interphase between the metal surface and corrosive agent. The mechanism of adsorption can either be by chemical or physical means via the adsorbed blanketing or protective layer which blocks the interphase or region between the metal surface and corrosive agent either by mono or double layer formation. Availability of different functional groups and structural arrangements within the molecular structure of corrosion inhibitor is possible through mixing or combining different materials together and the material obtained or produced is technically regarded as a composite material. This enables the inhibiting species to have more interactions with the charge on the metal surface, thereby promoting more surface coverage due to enhanced protection from the stability of adsorption and corroded product. The existing interaction between the charge on the surface of carbon steel and inhibiting species of SP and PVP respectively contributed immensely in forming a complex protective film that retarded the dissolution of carbon steel in 1 M $H_2SO_4$ environment in this research. Also, the blend or mixture SP and PVP showed a remarkable reduction in the damage done by the corrosive action and the improvement in the inhibition efficiency recorded was far more appreciative when either SP or PVP was used alone. Probably, this suggests that having multiple inhibiting species or groups within the corrodent system containing metal enhances the level at which the metal will be protected.

## 10 Conclusion

Soy polymer (SP) from soybean and PVP were found to be near-excellent inhibitors from polymer sources for carbon steel corrosion in an unfavourable environment. The inhibition of carbon steel corrosion in 1 M $H_2SO_4$ environment by SP and PVP respectively occurred by adsorption via the Langmuir adsorption isotherm. The efficiency of inhibition increased with a corresponding increment in concentration and decreased with a rise in temperature, thus suggesting concentration dependence and physical adsorption respectively. The values of corrosion activation energy and heat of adsorption are higher in inhibiting solution compared to blank, thus supporting the proposed physical adsorption mechanism. It is observed that blends or mixtures of SP

and PVP showed better improvement in inhibition effectiveness when either SP or PVP was used alone. Polarization result showed that SP and PVP altered both anodic and cathodic reaction and acted as mixed inhibitors based on the fact the displacement in corrosion potential caused by the addition of individual inhibitor does not exceed 85 mV. Quantum chemical calculations confirm the ability of protein and polyvinylpyrrolidone molecule respectively to adsorb on a carbon steel surface.

**Acknowledgement** The assistance received from the Department of Polymer and Textile Engineering, National Metallurgical Development Centre Zaria Road, Jos, Nigeria, Electrochemistry and Materials Science Research Laboratory, Department of Chemistry, Federal University of Technology, Owerri, Nigeria in making this work successful is acknowledged by the authors.

## Compliance with ethical standards

**Conflict of interest** On behalf of all authors, the corresponding author states that there is no conflict of interest.

## References

1. El-Shamy HF, Aggour YA, Ahmed AM (2017) Study the metallic finishing and corrosion control processes for carbon steel over head pipes using polymer molecules. MOJ Biorg Org Chem 1(5):1–11
2. Rani BEA, Basu BBJ (2012) Green inhibitors for corrosion protection of metals and alloys: an overview. Int J Corros 38:105–120
3. Umoren SA (2009) Polymers as corrosion inhibitors for metals in different media—a review. Open Corros J 2:175–188
4. Rajendran S, Sridevi SP, Anthony N, Amairaj AJ (2005) Corrosion behaviour of carbon steel in polyvinyl alcohol. Anti Corros Methods Mater 52:102–107
5. Yurt A, Butun V, Duran B (2007) Effect of the molecular weight and structure of some novel water-soluble triblock copolymers on the electrochemical behaviour of mild steel. Mater Chem Phys 105:114–121
6. Umoren SA, Ebenso EE, Okafor PC, Ogbobe O (2006) Water soluble polymers as corrosion inhibitors of mild steel in acidic medium. Pigment Resin Technol 35:346–352
7. Umoren SA, Ebenso EE (2008) Blends of polyvinyl pyrrolidone and polyacrylamide as corrosion inhibitors for aluminium in acidic medium. Ind J Chem Technol 15:355–363
8. David EA, Achika J, Ameh PO, Anya C (2013) A review on the assessment of polymeric materials used as corrosion inhibitor of metals and alloys. Int J Ind Chem 4(2):2–9
9. Chike-Onyegbula CO, Obasi HC, Ezeamaku UL, Azubuike L (2017) Corrosion inhibition and adsorption properties of soy polymer extract of glycine mac-L on mild steel in acidic medium. Eur J Adv Eng Tech 4(9):657–662
10. Ogundiran RK (2004) Soybean production and industrial utilization. In: 25th International conference on industrial processing of soybean, Nigeria
11. Nwanonenyi SC, Obasi HC, Chidiebere AM (2018) Inhibitive performance of carboxymethyl cellulose and additives on corrosion of carbon steel in acidic and alkaline environments. J Bio Tribo Corros 4:31
12. Hassan RM, Ishaq AZ (2013) Kinetics of corrosion inhibition of aluminium in acidic media by water-soluble natural polymeric pectates as anionic polyelectrolyte inhibitors. Materials 6:2436–2451
13. Cruz J, Pandiyan T, Ochoa EG (2005) A new inhibitor for mild carbon steel, electrochemical and DFT studies. J Electroanal Chem 583:8–16
14. Bartley J, Huynh N, Bottle SE, Flitt H, Notoya T, Schweinsberg DP (2003) Computer simulation of the corrosion inhibition of copper in acidic solution by alkyl esters of 5-carboxybenzotriazole. Corros Sci 45:81–96
15. Rodríguez-Valdez LM, Martinez-Villafane A, Glossman-Mitnik D (2005) Computer simulation of the molecular structure and properties of heterocyclic organic compounds with possible inhibition properties. J Mol Struct Theochem 713:65–70
16. Oguzie EE (2007) Corrosion inhibition of aluminium in acidic and alkaline media by *Sansevieria trifasciata* extract. Corros Sci 49:1527–1539
17. Nwanonenyi SC, Ogbobe O, Oguzie EE (2017) Protection of mild steel corrosion in sulphuric acid environment using wheat starch. Int J Eng Technol 10:11–21
18. Nwanonenyi SC, Ogbobe O, Madufor IC, Oguzie EE (2016) Influence of polyvinyl acetate on corrosion inhibition of mild steel in the sulphuric acidic environment. Eur J Adv Eng Tech 3:52–61
19. Nwanonenyi SC, Madufor IC, Uzoma PC, Chukwujike IC (2016) Corrosion inhibition of mild steel in the sulphuric acid environment using millet starch and potassium iodide. IUPAC 12:1–15
20. Onuchukwu AI (1988) Corrosion inhibition of aluminium in alkaline medium. I: Influence of hard bases. Mater Chem Phys 20(4–5):323–332
21. Aytac A, Ozmen U, Kabasakaloglu M (2005) Investigation of some Schiff bases as acidic corrosion of alloy AA3102. Mater Chem Phys 89:176–181
22. Ebenso EE, Oguzie EE (2005) Corrosion inhibition of mild steel in acidic media by some organic dyes. Mater Lett 59:2163–2165
23. Obot IB, Umoren SA, Obi-Egbedi NO (2011) Corrosion inhibition and adsorption behaviour for aluminium by an extract of *Aningeria robusta* in HCl solution: synergistic effect of iodide ions. J Mater Environ Sci 2(1):60–71
24. Umoren SA, Solomon MM, Udosoro II (2010) Synergistic and antagonistic effects between halide ions and carboxymethyl cellulose for the corrosion inhibition of mild steel in sulphuric acid solution. Cellulose 17:635–648
25. Nwanonenyi SC, Arukalam IO, Obasi HC, Ezeamaku UL, Eze IO, Chukwujike IC, Chidiebere MA (2017) Corrosion inhibitive behaviour and adsorption of millet (*Panicum miliaceum*) starch on mild steel in the hydrochloric acid environment. J Bio Tribo Corros 3:54. https://doi.org/10.1007/s40735-017-0115-y
26. Hazwan MH, Kassim MJ (2010) Corrosion inhibition and adsorption behaviour of *Uncaria gambir* extract on mild steel in 1 M HCl. Mater Chem Phys. https://doi.org/10.1016/j.matchemphys.2010.10.032
27. Avci G (2008) Inhibitor effect of *N*, *N*-methylenediacrylamide on corrosion behaviour of mild steel in 0.5 M HCl. Mater Chem Phys 112:234–238
28. Umoren SA, Obot IB, Ebenso EE, Obi-Egbedi NO (2009) The inhibition of aluminium corrosion in hydrochloric acid solution by exudate gum from *Raphia hookeri*. Desalination 247:561–572
29. Bahrami MJ, Hosseini SMA, Pilvar P (2010) Experimental and theoretical investigation of organic compounds as inhibitors for mild steel corrosion in the sulfuric acid medium. Corros Sci 52:2793–2803
30. Özcan M, Karadag F, Dehri I (2008) Interfacial behaviour of cysteine between mild steel and sulfuric acid as a corrosion inhibitor. Acta Phys Chim Sin 24:1387–1393
31. Torresi RM, Solange S, Pereira da Silva JE, Susana I, Torresi C (2005) Galvanic coupling between the metal substrate and

polyaniline acrylic blends: corrosion protection mechanism. Electrochim Acta 50:2213–2218
32. Bressy-Brondino C, Boutevin B, Hervaud Y, Gaboyard M (2002) Adhesive and anticorrosive properties of poly (vinylidene fluoride) powders blended with phosphonate copolymers on galvanized steel plates. J Appl Polym Sci 83:2277–2287
33. Ferreira ES, Giancomelli C, Giancomelli FC, Spinelli A (2004) Evaluation of the inhibitor effect of L-ascorbic acid on the corrosion of mild steel. Mater Chem Phys 83:129–134
34. Onuchukwu AI, Baba AI (1987) A study of the effects df ionogen on the corrosion stripping of the ZN surface of galvanized steel in an aqueous medium. Mater Chem Phys 18(4):381–390
35. Umoren SA, Obot IB, Ebenso EE, Okafor PC, Ogbobe O, Oguzie EE (2009) Gum arabic as a potential corrosion inhibitor for aluminium in alkaline medium and its adsorption characteristics. Anti Corros Methods Mater 53:517
36. Chidiebere MA, Nwanonenyi S, Njoku D, Iroha NB, Oguzie EE, Li Y (2017) Experimental study on the inhibitive effect of phytic acid as a corrosion inhibitor for Q235 mild steel in 1 M HCl environment. World News Nat Sci 15(2017):1–19
37. Akalezi CO, Onyedika GO, Chahul HF, Oguzie EE (2016) Experimental and theoretical studies on the corrosion inhibition of mild steel in acidic media by *Pentaclethra macrophylla* plant extract. FUTOJNLS 2(1):265–280
38. Ju H, Zhen-peng K, Li Y (2008) Aminic nitrogen-bearing polydentate Schiff base compounds as corrosion inhibitors for iron in acidic media: a quantum chemical calculation. Corros Sci 50:865–871
39. Udhayakala P (2014) Density functional theory calculations on corrosion inhibitory action of five azlactones on mild steel. J Chem Pharm Res 6(7):117–127
40. Martinez S, Stagljar I (2003) Correlation between the molecular structure and the corrosion inhibition efficiency of chestnut tannin in acidic solutions. J Mol Struct (Theochem) 640(1–3):167–174
41. Lukovits I, Kalman E, Zucchi F (2001) Corrosion inhibitors-correlation between electronic structure and efficiency. Corrosion 57:3–8